J Electr Eng Technol.2018; 13(1): 211-219
http://doi.org/10.5370/JEET.2018.13.1.211

ISSN(Print) 1975-0102
ISSN(Online) 2093-7423

PSO-Based Nonlinear PI-type Controller Design for Boost Converter

Sang-Wha Seo*, Yong Kim* and Han Ho Choi†

Abstract – This paper designs a nonlinear PI-type controller for the robust control of a boost DC-DC converter using a particle swarm optimization (PSO) algorithm. Based on the common knowledge that the transient responses can be improved if the P and I gains increase when the transient error is big, a nonlinear PI-type control design method is developed. A design procedure to autotune the nonlinear P and I gains is given based on a PSO algorithm. The proposed nonlinear PI-type controller is implemented in real time on a Texas Instruments TMS320F28335 floating-point DSP. Simulation and experimental results are given to demonstrate the effectiveness and practicality of the proposed method.

Keywords: Particle swarm optimization (PSO), PI control, Boost converter, Uncertainty, Nonlinear system

1. Introduction

DC-DC converters have been popular in many industrial applications due to its small size and high power density. It should be noted that the electric power output is usually delivered at the output voltage range of 12 to 80 V_{DC} in renewable energy sources such as PV modules, wind turbines, full cells, and battery systems. In order to satisfy the electric grid standards the output voltage value should be increased to the system DC bus voltage of around 200 or 400 V_{DC} depending on the AC load and grid requirements (Refer to Fig. 1)[1, 2]. DC-DC converter control systems usually undergo nonlinearities as well as parameter variations. And this leads to significant control performance degradation. For precise control of DC-DC converters under nonlinearities or uncertainties many researchers have developed numerous advanced methods, e.g. nonlinear control [3, 4], sliding mode control [5-8], fuzzy control [9-12], adaptive control [13]. These advanced methods give good transient and steady-state control performances. However, the conventional PI-type control methods are still widely used because they are very simple and they give comparable performances as shown in [9]. Considering this fact, we propose a nonlinear PI-type control system design method for DC-DC boost converter systems. Reflecting on the common control engineering knowledge [9, 12] that the transient responses can be improved if the P and I gains increase when the transient error is big, we design nonlinear P and I gains. We assume that the nonlinear P and I gains can be represented by using weighted sums of Gaussian functions of which values become larger as the output error increases. We cast the problem of designing the nonlinear PI-type controller as a nonlinear optimization problem. And we give a PSO-based procedure to solve the design problem. We implement the nonlinear PI-type control algorithm on a Texas Instruments TMS320F28335 floating-point DSP and we give simulation and experimental results verifying that the proposed nonlinear PI-type controller gives smaller overshoot and faster recovery time than a conventional PI-type controller.

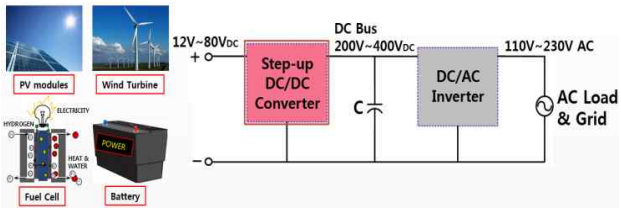

Fig. 1. Renewable energy system with integrated DC-DC boost converter

This paper is organized as follows. Section 2 gives an mathematical description of a boost converter. Section 3 presents a conventional PI-type controller design method based on the boost converter model. Section 4 gives a nonlinear PI-type controller and analyzes the closed-loop stability. Section 5 proposes a PSO-based algorithm to optimize the nonlinear PI control gains under some performance criteria. Section 6 shows the practicality and effectiveness of the proposed design method via simulation and experimental results. Section 7 gives some concluding remarks.

2. System Description

A boost DC-DC converter can be described by the following second-order nonlinear dynamic Eq. (3, 4).

† Corresponding Author: Div. of Electrical and Electronic Engineering, Dongguk Univ.-Seoul, Korea. (hhchoi@dongguk.edu)
* Div. of Electrical and Electronic Engineering, Dongguk Univ.-Seoul, Korea. ({20131157, kyee}@dongguk.edu)
Received: November 22, 2016; Accepted: September 1, 2017

$$\begin{aligned} \dot{i}_L &= -\frac{1}{L}v_C + \frac{1}{L}v_C u + \frac{E}{L} \\ \dot{v}_C &= \frac{1}{C}i_L - \frac{1}{RC}v_C - \frac{1}{C}i_L u \end{aligned} \tag{1}$$

where $\dot{i}_L$, v_C, u denote the input inductor current, the output capacitor voltage, the duty ratio input function ranging on the interval [0, 1]. The symbols *E, L, C, R* represent the external source voltage value, the input circuit inductance, the output filter capacitance, the output load resistance, respectively.

We will use the following assumptions:

A1 : $\dot{i}_L$, v_C, are available.

A2 : The inductor current is never allowed to be zero, i.e. the converter is in continuous conduction mode.

By introducing the following error terms

$$z_1 = i_L - \frac{V_r^2}{RE},\ z_2 = v_C - V_r,\ z_3 = \int_0^t (v_C - V_r)d\tau = \int_0^t z_2 d\tau,$$
$$v = 1 - u - \frac{E}{V_r}$$

we can obtain the following error dynamics from (1)

$$\dot{z} = Az + Bv + \Delta Bv \tag{2}$$

where $\dot{z} = \left[z_1, z_2, z_3\right]^T$, V_r is the desired reference output voltage satisfying $V_r > E > 0$, and

$$A = \begin{bmatrix} 0 & -\frac{E}{LV_r} & 0 \\ \frac{E}{CV_r} & -\frac{1}{RC} & 0 \\ 0 & 1 & 0 \end{bmatrix},\ B = \begin{bmatrix} -\frac{V_r}{L} \\ \frac{V_r^2}{RCE} \\ 0 \end{bmatrix},\ \Delta B = \begin{bmatrix} -\frac{z_2}{L} \\ \frac{z_1}{C} \\ 0 \end{bmatrix} \tag{3}$$

After all, our design problem can be formulated as proposing a stability analysis and control synthesis method for the error dynamics (2). Fig. 2 shows a block diagram of the PI controller for a boost converter.

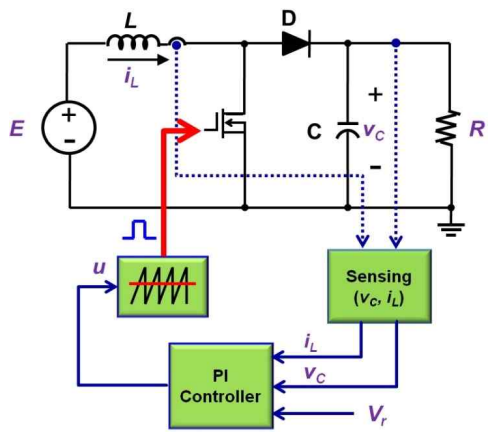

Fig. 2. Closed-loop boost converter control system

3. Conventional PI-type Controller

The nonlinear model (2) can be linearized at the operating point $z = 0$ as follows:

$$\dot{z} = Az + Bv \tag{4}$$

Assume that the control input *v* is given by the following PI-type control law

$$v = K_1 z_1 + K_P e + K_I \int_0^t e d\tau \tag{5}$$

where K_1, K_P, K_I are gains, especially K_P and K_I are the P and I gains, and e is the output error, i.e. $e = v_C - V_r = z_2$. Then the control law (5) can be rewritten as

$$\begin{aligned} v &= K_1 z_1 + K_P z_2 + K_I \int_0^t z_2 d\tau = K_1 z_1 + K_P z_2 + K_I z_3 \\ &= \left[K_1, K_P, K_I\right] z = Kz \end{aligned} \tag{6}$$

and the linearized system model (4) with the above PI-type control law leads to the following closed-loop system dynamics

$$\dot{z} = A_{cl} z = (A + BK)z \tag{7}$$

where the system matrix A_{cl} is given by

$$A_{cl} = \begin{bmatrix} -\frac{V_r}{L}K_1 & -\frac{E}{LV_r} - \frac{V_r}{L}K_P & -\frac{V_r}{L}K_I \\ \frac{V_r^2}{RCE}K_1 + \frac{E}{CV_r} & -\frac{1}{RC} + \frac{V_r^2}{RCE}K_P & \frac{V_r^2}{RCE}K_I \\ 0 & 1 & 0 \end{bmatrix} \tag{8}$$

This yields the following characteristic polynomial

$$\Delta_3(s) = \det(sI - A_{cl}) = s^3 + \alpha_2 s^2 + \alpha_1 s + \alpha_0 \tag{9}$$

where the coefficients α_0, α_1 and α_2 are given by

$$\begin{aligned} \alpha_0 &= \frac{E}{LC}K_I \\ \alpha_1 &= \frac{2V_r}{RC}K_1 + \frac{E}{LC}K_P - \frac{V_r^2}{RCE}K_I + \frac{E^2}{LCV_r^2} \end{aligned} \tag{10}$$

$$\alpha_2 = \frac{V_r}{L}K_1 - \frac{V_r^2}{RCE}K_P + \frac{1}{RC}$$

The polynomial (9) implies that the closed-loop control system matrix A_{cl} is stable if the gains K_1, K_P, and K_I satisfy the inequality condition [13]

$$(\frac{V_r}{L}K_1 - \frac{V_r^2}{RCE}K_P + \frac{1}{RC})(\frac{2V_r}{RLC}K_1 + \frac{E}{LC}K_P - \frac{V_r^2}{RCE}K_I + \frac{E^2}{LCV_r^2}) > \frac{E}{LC}K_I \quad (11)$$

It should be noted that for $K_1 = K_I = 0$ and $K_P = E/2V_r^2$ the above stability condition (11) is trivially satisfied and thus it is always feasible, i.e. the linearized system model of the boost DC-DC converter is always stabilizable with a PI-type control law. Since the Lyapunov's linearization method implies that the original nonlinear system is stable as long as the linearized system is stable, we can stabilize the nonlinear boost model (2) by using the PI-type controller (6) satisfying the condition (11).

4. Nonlinear PI-type Controller

The common control engineering knowledge [9, 12] implies that the control performances can be enhanced if the P and I gains are replaced with larger values when the error is big, thus we can improve control performances of the conventional controller (6) by slightly increasing the P and I gains as the output error grows. To this end, we modify the conventional PI-type control law (6) and we consider the following nonlinear PI-type controller :

$$v = K_1 z_1 + K_P\left[1 + \delta_P(1 - \sum_{j=1}^{N}\varphi_j e^{-\eta_j z_2^2})\right]z_2 + K_I\left[1 + \delta_I(1 - \sum_{j=1}^{N}\rho_j e^{-\zeta_j z_2^2})\right]\int_0^t z_2 d\tau \quad (12)$$

where N is some integer, $\delta_P, \delta_I, \varphi_j, \eta_j, \rho_j, \zeta_j$ are nonnegative constants. We will assume that φ_j, η_j can be represented by using nonnegative design parameters

$$\varphi_j = \phi_j\left[\sum_{i=1}^{N}\phi_i\right]^{-1}, \rho_j = \sigma_j\left[\sum_{i=1}^{N}\sigma_i\right]^{-1} \quad (13)$$

which will guarantee

$$\sum_{j=1}^{N}\varphi_j = \sum_{j=1}^{N}\sigma_j = 1 \quad (14)$$

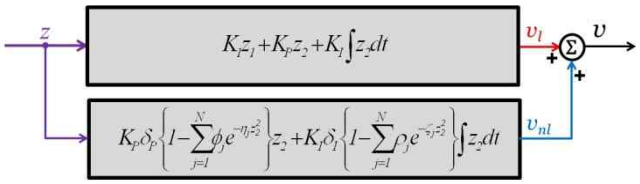

Fig. 3. Block diagram of the nonlinear PI-type controller

It should be noted that the above nonlinear PI-type controller (12) can be rewritten as the summation of the linear part v_l and the nonlinear part v_{nl}

$$v = v_l + v_{nl} \quad (15)$$

where the linear part v_l is the same as the conventional linear PI-type control law (6) and the nonlinear part v_{nl} is given by

$$v_{nl} = K_P\left[\delta_P(1 - \sum_{j=1}^{N}\varphi_j e^{-\eta_j z_2^2})\right]z_2 + K_I\left[\delta_I(1 - \sum_{j=1}^{N}\rho_j e^{-\zeta_j z_2^2})\right]\int_0^t z_2 d\tau \quad (16)$$

Fig. 3 shows a block diagram of the nonlinear PI-type control law of (12).

It should be noted that an excessively large gain value will lead to violation of hardware constraints. The gains of the proposed nonlinear PI-type control law (12) are positive reverse bell-shaped nonlinear functions and thus the gains are confined in some ranges. If the output voltage error $e = z_2$ becomes small then by (14) the followings can be obtained

$$\sum_{j=1}^{N}\varphi_j e^{-\eta_j z_2^2} \approx \sum_{j=1}^{N}\varphi_j = 1, \ \sum_{j=1}^{N}\rho_j e^{-\zeta_j z_2^2} \approx \sum_{j=1}^{N}\rho_j = 1 \quad (17)$$

leading to $v_{nl} \approx 0$. Thus the above nonlinear PI-type control law (12) can be approximated by the linear PI-type control law (6) when the error is small. If the output voltage error e is big, i.e. $|e| \gg 1$ then the nonlinear functions $\sum_{j=1}^{N}\varphi_j e^{-\eta_j z_2^2}$ and $\sum_{j=1}^{N}\rho_j e^{-\zeta_j z_2^2}$ go to zero and

$$v_{nl} \approx K_P\delta_P z_2 + K_I\delta_I\int_0^t z_2 d\tau \quad (18)$$

thus the above nonlinear PI-type control law (12) can be approximated by the following linear PI-type control law (6) with bigger gains than those of (6) :

$$v = K_1 z_1 + K_P\left[1 + \delta_P\right]z_2 + K_I\left[1 + \delta_I\right]\int_0^t z_2 d\tau \quad (19)$$

We can see that the P gain of our nonlinear PI-type controller is within the range $[K_P,\ K_P\ (1+\delta_P\ )]$ and the I gain is within $[K_I,\ K_I\ (1+\delta_I\ )]$. Using (12), and referring to (7) and (8) we can obtain the following error dynamics :

$$\dot{z}=\begin{bmatrix} -\frac{V_r}{L}K_1 & -\frac{E}{LV_r}-\frac{V_r}{L}\kappa_P & -\frac{V_r}{L}\kappa_I \\ \frac{V_r^2}{RCE}K_1+\frac{E}{CV_r} & -\frac{1}{RC}+\frac{V_r^2}{RCE}\kappa_P & \frac{V_r^2}{RCE}\kappa_I \\ 0 & 1 & 0 \end{bmatrix} z \quad (20)$$

where

$$\kappa_P = K_P\left(\delta_P(1-\sum_{j=1}^{N}\varphi_j e^{-\eta_j z_2^2})\right)\in\left[K_P, K_P\left(1+\delta_P\right)\right],$$

$$\kappa_I = K_I\left[\delta_I(1-\sum_{j=1}^{N}\rho_j e^{-\zeta_j z_2^2})\right]\in\left[K_I, K_I\left(1+\delta_I\right)\right]$$

The above error dynamics (19) yields the following third-order characteristic function

$$s^3+b_2s^2+b_1s+b_0 \quad (21)$$

where

$$b_0\in\left[\frac{E}{LC}K_I, \frac{E}{LC}K_I(1+\delta_I)\right],\ b_1\in\left[b_{1m}, b_{1M}\right]$$

$$b_2\in\left[\frac{V_r}{L}K_1-\frac{V_r^2}{RCE}K_P(1+\delta_P)+\frac{1}{RC}, \frac{V_r}{L}K_1-\frac{V_r^2}{RCE}K_P+\frac{1}{RC}\right]$$

and

$$b_{1m}=\frac{2V_r}{RC}K_1+\frac{E}{LC}K_P-\frac{V_r^2}{RCE}K_I(1+\delta_I)+\frac{E^2}{LCV_r^2}$$

$$b_{1M}=\frac{2V_r}{RC}K_1+\frac{E}{LC}K_P(1+\delta_P)-\frac{V_r^2}{RCE}K_I+\frac{E^2}{LCV_r^2}$$

By using the previous result on the Kharitonov's theorem [13], we can see that the characteristic function (20) with (21) is asymptotically stable if

$$b_{1M}\left[\frac{V_r}{L}K_1-\frac{V_r^2}{RCE}K_P(1+\delta_P)+\frac{1}{RC}\right]>\frac{E}{LC}K_I(1+\delta_I) \quad (22)$$

This proves the following theorem.

Theorem 1 Consider the closed-loop system of the linearized system model (4) with the proposed nonlinear PI-type control law (12). Then, the asymptotic stability of $z=0$ is guaranteed as long as the control parameters $K=[K_1, K_P, K_I]$, δ_P, δ_I satisfies the condition (22).

Remark 1 It should be noted that the boost converter (1) can be stabilized by the proposed nonlinear PI-type controller (12) if the control parameters $K=[K_1, K_P, K_I]$, δ_P, δ_I are tuned by using the condition (22)

5. Particle Swarm Optimization Algorithm to Autotune Nonlinear PI Controller

The control performances of the proposed nonlinear PI-type controller (12) will depend on the value of the parameter vector $\psi=[\varphi^T, \eta^T, \sigma^T, \zeta^T]^T\in R^{4N}$ where $\varphi=[\varphi_1, \cdots, \varphi_N]^T$, $\eta=[\eta_1, \cdots, \eta_N]^T$, $\sigma=[\sigma_1, \cdots, \sigma_N]^T$, and $\zeta=[\zeta_1, \cdots, \zeta_N]^T$. Thus it is reasonable to find some optimal vector ψ minimizing a performance criterion for the given K_1, K_P, K_I, δ_P, and δ_I satisfying the stability condition (22). Because the index ISE is one of the most popular measures to compare the control performances of PID control systems, we will consider the following integral performance index J to find the optimal ψ

$$J=\int_0^{t_f} e^2 dt \quad (23)$$

where t_f is the final time.

After all, the nonlinear PI-type control design problem can be cast as an optimization problem of finding the optimal parameter vector ψ such that the integral performance index J is minimized for the given gain $K=[K_1, K_P, K_I]$. The optimization problem can be rewritten as

$$\mathrm{P}: \arg\max_{\psi} J(\psi) \quad subject\ \ to\ \ (2),(12) \quad (24)$$

The optimization problem P of (24) is nonlinear and it seems difficult to solve analytically thus we try to use a PSO algorithm to find the optimal parameter vector ψ. In order to attack nonlinear problems many researchers have proposed bio-inspired evolutionary algorithms such as genetic algorithm and PSO. Numerous successful applications of PSO to solve difficult optimization problems have been reported in the literature [14-19]. In PSO, particles are used to represent trial solutions and a swarm of particles denotes the population of trial solutions. Each particle has two main attributes : position and velocity. PSO requires fewer parameters and it is simpler than other bio-inspired evolutionary algorithms such as genetic algorithm. A PSO algorithm is usually implemented by using the following steps :

S1 : Generate the initial particles with random position

and velocity values in the search space.
S2 : Evaluate the objective function of particles.
S3 : For each particle, compare the particle's objective function value with its previous best value. If the current position outperforms its previous best position, update it.
S4 : Find the global best position among the particle's previous best positions.
S5 : Update particles' velocities and positions.
S6 : Repeat steps 2 through 5 until a stopping criterion is satisfied.

In this section, we will develop an autotuning method for the control parameter vector ψ of the nonlinear PI-type controller (12) based on PSO approach.

5.1 Initialization

Before we actually start to optimize and autotune the control parameter vector ψ, we need to set the essential parameters of the maximum generation number G_{max} and the swarm size N_p. In the literature the swarm size is in the range 20 through 60.We cannot expect that a larger swarm size improves drastically the optimal value. This paper uses N_p=20. In the initialization step, we also create the N_p initial position vectors $p_i^{(0)} = [p_{i1}^{(0)}, p_{i2}^{(0)}, \cdots, p_{i4N}^{(0)}]^T$ and velocity vectors $v_i^{(0)} = [v_{i1}^{(0)}, v_{i2}^{(0)}, \cdots, v_{i4N}^{(0)}]^T$. We set $p_{ij}^{(0)}$ as random numbers taken from (0 10] and we use $v_i^{(0)} = 0$.

5.2 Objective function

The objective function is also called as the fitness function. This paper uses the integral performance index J of (23) as the objective function. For given k-th generation, each particle is evaluated for the objective function value under $\psi = p_i^{(k)}$. If the position $p_i^{(k)}$ is better than the personal best position p_i^* ever found by the i-th particle, set $p_i^* = p_i^{(k)}$. If the position $p_i^{(k)}$ is better than the global best position g^* found by any particle, set $g^* = p_i^{(k)}$.

5.3 Update Law

The updates of velocity and position are key operations in PSO. By using the following elementary floating point arithmetics the velocity and position are updated and a new swarm of particles is generated

$$v_i^{(k+1)} = Wv_i^{(k)} + \xi_1 r_1 (p_i^* - p_i^{(k)}) + \xi_2 r_2 (g^* - p_i^{(k)}) \tag{25}$$

$$p_i^{(k+1)} = \begin{cases} p_{\max} & If \quad p_i^{(k)} + v_i^{(k+1)} > p_{\max} \\ p_i^{(k)} + v_i^{(k+1)} & If \ p_{\min} \le p_i^{(k)} + v_i^{(k+1)} \le p_{\max} \\ p_{\min} & If \quad p_i^{(k)} + v_i^{(k+1)} \le p_{\min} \end{cases} \tag{26}$$

where p_{max} and p_{min} are some constants, W is the inertia weight coefficient, ξ_1 is the personal influence weight coefficient, and ξ_2 is the social influence weight coefficient. The terms r_1 and r_2 are uniformly distributed random numbers within [0, 1]. The vector p_i^* is the best position of the ith particle. The vector g^* denotes the global best position of the whole swarm. The first term of (25) gives the momentum for the particles to fly through the whole search space. The second term represents experience of an individual particle and it drives the particles to move toward their own best position. The third term represents the collaborative effect of the swarm in searching the global best. The inertia weight coefficient W controls the search range. A larger W enables the particles to search the optimal solution more globally. By decreasing the inertia weight W we can reduce the search space. We use $W = 0.5$ in this paper. The coefficients ξ_1 and ξ_2 control the speed towards the personal best and global best. Small ξ_1 and ξ_2 will make the particles fly slowly towards the personal best and global best. And large ξ_1 and ξ_2 can make the swarm unstable. The coefficients ξ_1 and ξ_2 are usually set equally as a positive constant within (0, 4]. This paper uses $\xi_1 = \xi_2 = 0.3$. It should be noted that the use of the same weight coefficients may incur the premature convergence phenomenon in which each particle behaves very similarly and the diversity of the swarm is decreased. This premature convergence phenomenon can be solved by varying the weight coefficients as the previous methods of [18,19].

5.4 Stopping criteria

The minimum objective function value becomes smaller than a prescribed value or it converges, we terminate the

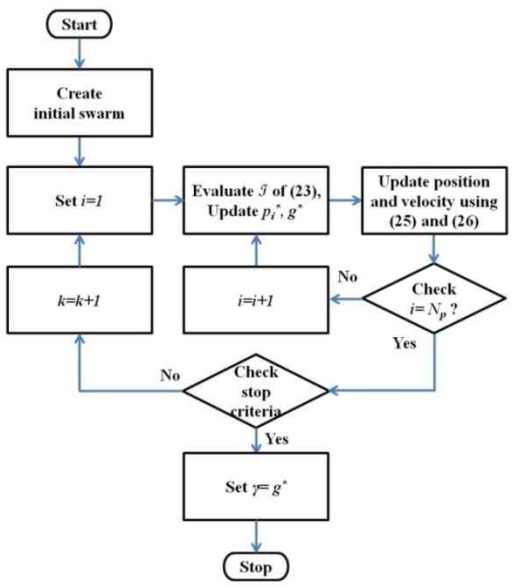

Fig. 4. PSO algorithm to autotune the nonlinear PI-type controller

algorithm. Alternatively, the maximum generation number G_m is reached, we stop, and we choose the global best position as the control parameter vector, i.e. $\psi = g^*$. Fig. 4 depicts a flow chart of the proposed PSO algorithm to autotune the control parameter vector ψ of the nonlinear PI-type control law (12).

6. Simulation and Experimental results

Consider a boost converter (1) with L=4[mH], C=300 [uF], E=64[V], the PWM switching frequency 40 [kHz]. Assume that the nominal load resistance is R= 1[kΩ] and the desired reference output voltage V_r is V_r = 200[V]. We assume that the input voltage E and the output load resistance R are within 48-80[V] and 333-1500[Ω], respectively. By using the result of [20], we can easily show that these design specifications can be satisfied with L=4[mH] as follows:

$$L_{\min} = \frac{2}{27}\frac{R_{\max}}{f_s} = \frac{2}{27}\frac{1500}{40\times 10^3} = 2.778mH \le 4mH = L$$

Similarly, we can show that the output filter capacitance C=300[uF] can meet the design specifications.

We assume that the input circuit inductance and the output filter capacitance are time-invariant whereas the load resistance is uncertain but bounded as (20). By referring to (2) and (3), we can obtain the following approximate averaged model

$$\dot{z} = \begin{bmatrix} 0 & -80 & 0 \\ 1066.7 & -3.333 & 0 \\ 0 & 1 & 0 \end{bmatrix} z + \begin{bmatrix} -\dfrac{v_C}{L} \\ \dfrac{i_L}{C} \\ 0 \end{bmatrix} v \qquad (27)$$

By referring to the analysis given in Section 3 or the existing methods of [2] and [7], we can design the following conventional linear PI-type controller for the above boost converter model

$$v = 0.1z_1 + 0.01z_2 + \int_0^t z_2 d\tau \qquad (28)$$

With the above linear PI-type controller, and N = 2, G_m = 50, N_p = 20, W = 0.5, $\xi_1 = \xi_2 = 0.3$, the following nonlinear PI-type controller is designed by the proposed PSO algorithm

$$\begin{aligned} v = {} & 0.1z_1 + 0.01\left(2 - 0.62e^{-1.71z_2^2} - 0.38e^{-1.56z_2^2}\right)z_2 \\ & + \left(2 - 0.12e^{-0.0163z_2^2} - 0.88e^{-0.016z_2^2}\right)\int_0^t z_2 d\tau \end{aligned} \qquad (29)$$

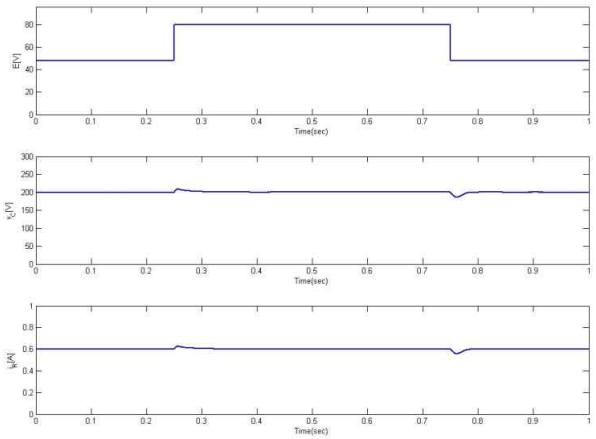

Fig. 5. Simulation results with the proposed method under C1

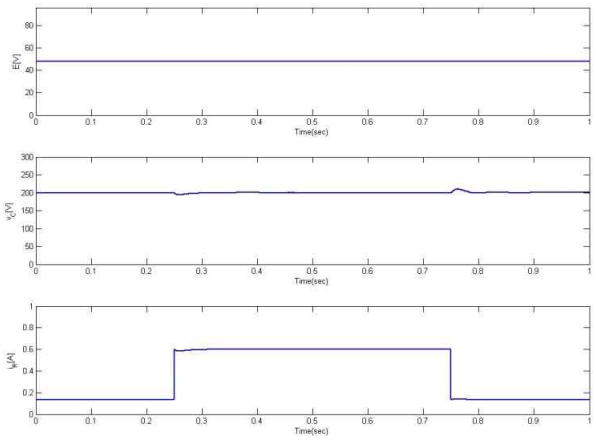

Fig. 6. Simulation results with the proposed method under C2

We consider the following two cases in order to verify the feasibility and practicality of the proposed method : Case 1) The external source voltage value E changes from 48[V] → 80[V] → 48[V] while the output load resistor is kept constant at R = 333[Ω]. Case 2) The output load resistor R changes from 1500[Ω] → 333[Ω] → 1500[Ω] while the external source voltage holds constant at E = 48 [V]. It should be noted that renewable energy sources such as photovoltaic module, fuel cell, or energy storage devices usually deliver output voltage within the range of 12 to 80 [V]. The boost converter (27) can be directly applied to step up the output voltages of the renewable energy sources. Fig. 5 shows the time trajectories of the input voltage E, the output voltage v_C, and the output current i_R subject to E changing abruptly from 48[V] → 80[V] → 48[V] with R = 333[Ω]. Fig. 6 illustrates the histories of E, v_C, and i_R when R changes abruptly from 1500[Ω] → 333[Ω] → 1500[Ω] while E holds constant at E = 48[V]. For some comparisons, we also consider the linear PI-type controller (28). Figs. 7 and 8 show the time histories by the conventional linear PI-type controller (28). Fig. 7 depicts the time histories of E, v_C, i_R when E changes

abruptly from 48[V] → 80[V] → 48[V] while R is kept constant at R = 333[Ω]. Fig. 8 shows the trajectories of E, v_C, and i_R subject to R changing abruptly from 1500[Ω] → 333[Ω] → 1500[Ω] with E=48[V]. Table 1 summarizes the comparative numerical results of the conventional controller (28) and the proposed controller (29). Table 1 and Figs. 5 through 8 imply that the proposed controller achieves 9.5 % reduction in integral of absolute output error, 11.1 % reduction in integral of squared output error, and 32.3 % reduction in integral of time-weighted squared output error, 50% reduction in percentage overshoot for the case C1 compared to the conventional controller (28). The proposed controller achieves 17.2 % reduction in integral of absolute output error, 28.5 % reduction in integral of squared output error, and 19.1 % reduction in integral of time-weighted squared output error, 50% reduction in percentage overshoot for the case C2 compared to the conventional controller.

Table 1. Numerical comparison between conventional controller and proposed controller.

		$\int_0^1 \lvert e \rvert dt$	$\int_0^1 e^2 dt$	$\int_0^1 te^2 dt$	% Overshoot
Conventional controller (28)	C1	0.5821	5.1103	2.6166	15
	C2	0.4971	3.0789	1.6477	10
Proposed controller (29)	C1	0.5269	3.8291	2.3274	7.5
	C2	0.4118	2.2017	1.3334	5

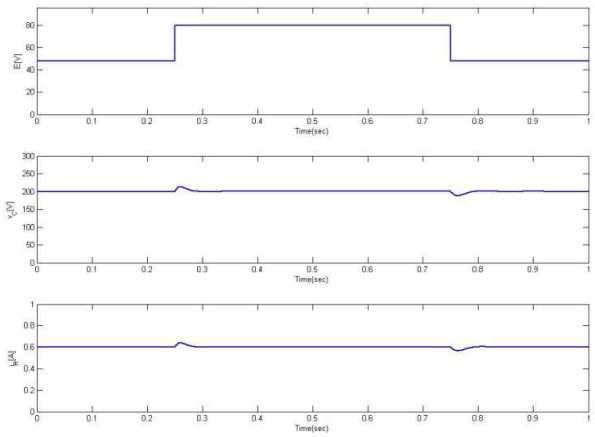

Fig. 7. Simulation results with the conventional method under C1

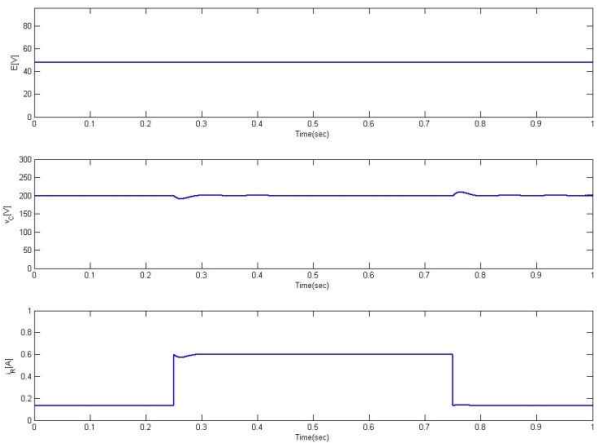

Fig. 8. Simulation results with the conventional method under C2

An experimental test setup is constructed to show the practicality and feasibility of the proposed method as shown in Fig. 9. The proposed control algorithm is implemented on a Texas Instruments TMS320F28335 floating-point DSP. The TMS320F28335 DSP supports real-time embedded control oriented features such as 16 12-bit ADC channels, two multichannel buffered serial port modules, three 32-bit timers, 34 KB RAM, 256 KB flash ROM, 8 external interrupts. By using a 12-bit ADC module with a built-in sample-and-hold circuit, the output capacitor voltage v_C is converted into a digital value for control input calculation. The output signal v_C is measured and depicted with a Tektrnonix TDS5104B digital oscilloscope. Figs. 10 through 13 illustrate the experimental results under the same conditions as Figs. 5 through 8, respectively. Figs. 5-

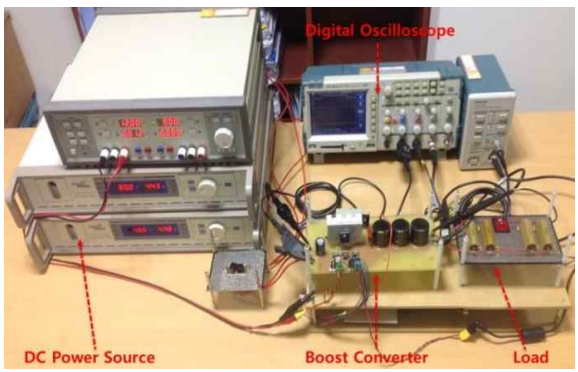

Fig. 9. Experimental test setup

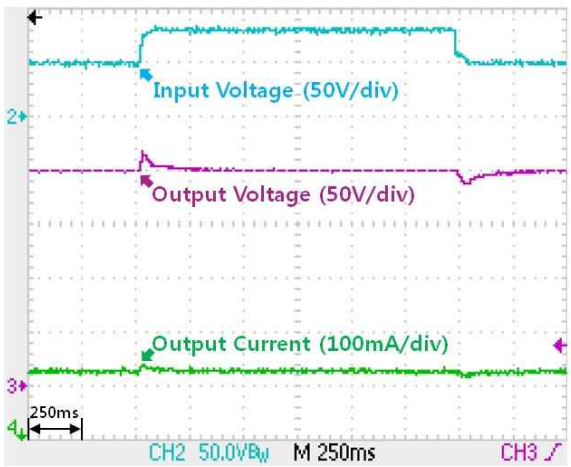

Fig. 10. Experimental results with the proposed method under C1

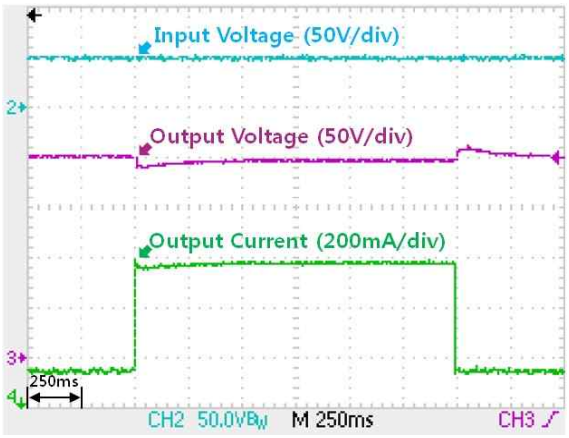

Fig. 11. Experimental results with the proposed method under C2

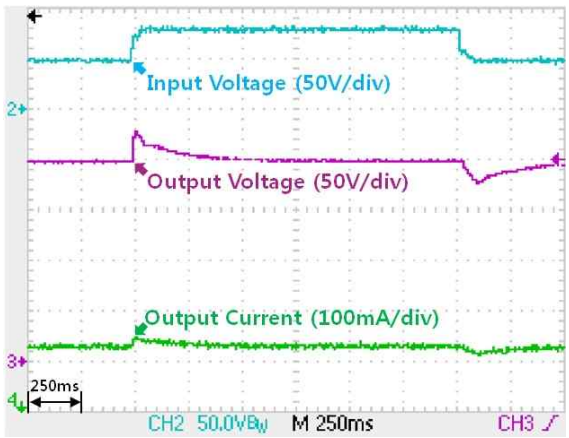

Fig. 12. Experimental results with the conventional method under C1

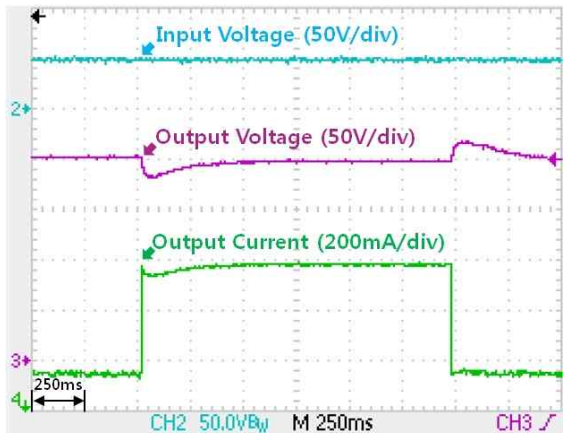

Fig. 13. Experimental results with the conventional method under C2

8 and Figs. 10-13 verify that the experimental results are well matched to the simulation results and the proposed nonlinear PI-type controller can be better than the conventional linear PI-type controller.

7. Conclusion Remarks

Based on a PSO algorithm a nonlinear PI-type control design method was proposed for a boost converter. The proposed nonlinear PI-type controller was designed by using the common control engineering knowledge that the transient control performance can be improved if the P and I gains increase as the error grows. We gave a PSO-based design procedure to optimize and autotune the nonlinear P and I gains. Finally, we verified the practicality and feasibility of the proposed method by using simulation and experiments.

Acknowledgment

This work was supported by the National Research Foundation of Korea(NRF) grant funded by the Korea government(MSIP) (No. 2014R1A2A1A11049543). This research was supported by Basic Science Research Program through the National Research Foundation of Korea (NRF) funded by the Ministry of Education (No. 2017R1D1A1B03030652). This work was supported by the Korea Institute of Energy Technology Evaluation and Planning(KETEP) and the Ministry of Trade, Industry & Energy(MOTIE) of the Republic of Korea [Grant Number. 20174030201520].

References

[1] H. Sira-Ramirez, R.A. Perez-Moreno, and M. Garcia-Esteban, "Passivity-based controllers for the stabilization of DC-to-DC power converters," *Automatica,* vol. 33, no. 4, pp. 499-513, 1997.

[2] G. Escobar, R. Ortega, and H. Sira-Ramirez, "An experimental comparison of several nonlinear controllers for power converters," *IEEE Contr. Syst. Magazine,* vol. 19, no. 1, pp. 66-82, 1999.

[3] H. Sira-Ramirez, "On the generalized PI sliding mode control of DC-to-DC power converters: A tutorial," *Int. J. Control*, vol. 76, pp. 1018-1033, 2003.

[4] S.K. Mazumder, A.H. Nayfeh, and D. Boroyevich, "Robust control of parallel dc/dc buck converters by combining integral-variable-structure and multiple-sliding-surface control schemes," *IEEE Tran. Power Elec.,* vol. 17, pp. 428-437, 2002.

[5] S.-C. Tan, Y. M. Lai, and C.K. Tse, "Indirect sliding mode control of power converters via double integral sliding surface," *IEEE Tran. Power Elec.,* vol. 23, pp. 600-611, 2008.

[6] S.K. Mazumder, and K. Acharya, "Multiple Lyapunov function based reaching criteria for orbital existence of switching power converters," *IEEE Tran. Power Elec.*, vol. 23, pp. 1449-1471, 2008.

[7] L. Guo, J.Y. Hung, and R.M. Nelms, "Evaluation of

DSP-based PID and fuzzy controllers for DC-DC converters," *IEEE Trans. Ind. Electron.* vol. 56, pp. 2237-2248, 2009.
[8] A.G. Perry, G. Feng, Y.F. Liu, and P.C. Sen, "A design method for PI-like fuzzy logic controllers for DC-DC converter," *IEEE Trans. Ind. Electron.,* vol. 54, pp. 345-355, 2007.
[9] K.-W. Seo, and H.H. Choi "Simple fuzzy PID controllers for DC-DC converters," *J. of Electrical Engineering & Technology,* vol. 7, pp.724-729, 2012.
[10] L. Guo, J.Y. Hung, and R.M. Nelms, "Design of a fuzzy controller usiing variable structure approach for application to DC-DC converters," *Electic Power Systems Research,* vol. 83, pp. 104-109, 2012.
[11] S. Oucheriah, and L. Guo, "PWM-based adaptive sliding-mode control for boost DC-DC converters," *IEEE Trans. Ind. Electron.,* vol. 60, pp. 3291-3294, 2013.
[12] Z.-Y. Zhao, Tomizuka, and S. Isaka, "Fuzzy gain scheduling of PID controllers," *IEEE Trans. Syst. Man Cybern.,* vol. 23, pp. 1392-1398, 1993.
[13] N.K. Bose, E.I. Jury, E. Zeheb, "On robust Hurwitz and Schur polynomials," *IEEE Trans. Automat. Contr.*, vol. 33, pp. 1166-1168, 1988.
[14] I. C. Trelea, "The particle swarm optimization algorithm: Convergence analysis and parameter selection," *Information Processing Letters.,* vol. 85, pp. 317-325, 2003.
[15] Y. Valle, G. K. Venayagamoorthy, S. Mohagheghi, J.-C. Herandez, and R.G. Harley "Particle swarm optimization : Basic concepts, variants and applications in power systems," *IEEE Trans. Evolutionary Computation*, vol. 12, pp. 171-195, 2008.
[16] M. R. AlRashidi and M. E. El-Hawary, "A survey of particle swarm optimization applications in electric power operations," *Electric Power Components and Systems*, vol. 34, no. 12, pp. 1349-1357, Dec. 2006.
[17] K. Parsopoulos and M. Vrahatis, "Recent approaches to global optimization problems through particle swarm optimization," *Natural Computing*, vol. 1, pp. 235-306, May 2002.
[18] Y, Shi, and R.C. Eberhart, "Empirical Study of Particle Swarm Optimization," Proceedings of Congress on Evolutionary Computation (CEC1999), 1999, pp. 1945-1950.
[19] P.J. Angeline "Using Selection to Improve Particle Swarm Optimization," *Proc. of IEEE International Conference on Evolutionary Computation, Anchorage, Alaska*, 1998, pp. 84-89.
[20] M.K. Kazimierczuk, and A. Massarini, "Feedforward control of DC-DC PWM boost converter," *IEEE Trans. Ind. Electron.*, vol. 44, no. 2, pp. 143-148, 1997.

Sang-Wha Seo received the B.S. degrees in electronic engineering from Seokyeong Univ., Seoul, Korea, in 2007 and M.S. degrees and Ph.D degrees in electrical engineering from Dongguk Univ.-Seoul, Korea, in 2010 and 2017. Since 2013, he has been with Dongguk university research institute for industrial technology.

Yong Kim received the B.S., M.S. degrees and Ph.D degrees in Department of Electrical Engineering from the Dongguk University in 1981, 1983 and 1994. Since 1995 He has been a Professor in the Div. of EEE, Dongguk Univ.-Seoul. His teaching and research interests include switch mode power supply and electrical motor drives.

Han Ho Choi received the B.S. degree in Control and Instrumentation Eng. from SNU, Seoul, Korea, and the M.S. and Ph.D. degree in Electrical Engineering from KAIST in 1988, 1990, and 1994, respectively. He is now with the Div. of EEE, Dongguk Univ.-Seoul.